Indian Geotech J (April–June 2014) 44(2):205–217
DOI 10.1007/s40098-013-0085-z

ORIGINAL PAPER

# Ground Engineering with Granular Inclusions for Loose Saturated Sands Subjected to Seismic Loadings

**A. Murali Krishna · M. R. Madhav · Kamlesh Kumar**

Received: 20 June 2012 / Accepted: 30 October 2013 / Published online: 12 November 2013


**Abstract** Sites having predominant loose sand deposits are prone to many hazards, especially under seismic loading conditions. Among different forms of seismic risks, liquefaction is being considered as a crucial hazard when the deposit is saturated/with high ground water level. Ground improvement methods are commonly employed to improve the natural site conditions under such situations for better performance of various engineering structures. Ground treatment by granular inclusions in columnar form can offer effective solution than most other ground improvement methods. This paper presents the review of various aspects of ground engineering of loose saturated sands with granular piles/stone columns. A short discussion on the seismic hazards associated with loose sand deposits with main focus on liquefaction followed by the outlines of the recent developments on the application of granular inclusions in the form of stone columns/granular piles as general ground improvement method as well as seismic hazard mitigation measure are presented. New design charts are developed based on pore pressure generation and dissipation considering various installation and behavioral effects and are discussed and compared with the original design curves. It is concluded that the granular inclusions are very effective in resisting the effects of seismic loading on loose saturated sands. It is also recommended to consider various affects of the granular inclusions together while designing the ground engineering system.

**Keywords** Earthquake engineering · Liquefaction · Ground improvement · Stone column · Drainage · Densification

A. Murali Krishna (✉) · K. Kumar
Department of Civil Engineering, Indian Institute of Technology Guwahati, Guwahati, India
e-mail: amurali@iitg.ernet.in

K. Kumar
e-mail: kamleshiitg7@gmail.com

M. R. Madhav
Department of Civil Engineering, Indian Institute of Technology Hyderabad & JNTU, Hyderabad, India
e-mail: madhavmr@gmail.com

## List of Symbols

| | |
|---|---|
| $a$ | Radius of the granular pile |
| $b$ | Radius of the unit cell |
| $k_h(r)$ | Horizontal permeability of treated ground at radial distance $r$ |
| $k_{hi}$ | Horizontal permeability of untreated ground |
| $m_v(r)$ | Coefficient of volume compressibility or treated ground at radial distance $r$ |
| $m_{vi}$ | Coefficient of volume compressibility or untreated ground |
| $N$ | Equivalent number of uniform stress cycles associated with any period of earthquake shaking |
| $N_{eq}$ | Equivalent number of uniform stress cycles induced by earthquake |
| $N_l$ | Number of uniform stress cycles required to cause liquefaction |
| $N_{eq}/N_l$ | Cyclic ratio |
| $R$ | Non-dimensionalized radial distance, $r/b$ |
| $r$ | Radial distance measured from the centre of granular pile |

| | |
|---|---|
| $T$ | Normalized time, $t/t_d$ |
| $t$ | Time |
| $T_{ad} = (k/\gamma_w)[t_d/(m_v a^2)]$ | Dimensionless time factor |
| $T_{bd} = (k/\gamma_w)[t_d/(m_v b^2)]$ | Dimensionless time factor |
| $T_s$ | Period of the earthquake shaking |
| $t_d$ | Duration of earthquake |
| $u$ | Excess hydrostatic pressure |
| $u_g$ | Excess hydrostatic pressure generated by earthquake shaking |
| $W$ or $r_u$ | Pore pressure ratio |
| $W_{\max}$ | Maximum pore pressure ratio $W$ throughout the layer at a given $T$ |
| $\sigma'_o$ | The initial mean bulk effective stress |
| $\alpha$ | A non-dimensional parameter describing the pore water pressure generation during shaking |

## Introduction

Sites having predominant loose sand deposits are prone to many hazards, especially under seismic conditions. One of the most dramatic causes of damage to structures during earthquakes has been the development of liquefaction in saturated loose sand deposits, manifested either by the formation of sand boils and mud-spouts at the ground surface, by seepage of water through ground cracks or in some cases by the development of quicksand conditions over substantial areas [1]. Liquefaction, the state under which soil deposit loses its strength and flows as a fluid is a major cause for damage during earthquakes. If the ground surface is inclined (sloping ground surface), liquefaction also leads to lateral spreading [2].

Ground improvement techniques are commonly employed to mitigate geotechnical seismic hazards i.e. liquefaction, foundation failures etc. Granular inclusions in the form of granular drains/piles or stone columns are the most widely preferred alternative all over the world, due to several advantages associated with them. Granular piles function as drains and permit rapid dissipation of earthquake induced pore pressures by virtue of their high permeability. In addition, they tend to dilate as they get sheared during an earthquake event. Seismic forces which tend to generate positive pore pressures in these deposits cause an opposite effect of dilation in dense granular piles. One of the chief benefits of ground treatment with granular piles is the densification of in situ ground by which the in situ properties of the ground get modified to mitigate the seismic risks especially, liquefaction potential. Further, the very high deformation modulus and stiffness of the granular pile material provide reinforcement for the in situ soil and offer another mechanism to mitigate liquefaction and participate in resisting lateral spreading. Thus, different mechanisms operate in the function of stone columns/granular piles in liquefaction mitigation. These mechanisms can be stated as drainage, storage, dilation, densification and reinforcement.

In this paper, a short discussion on the seismic hazards associated with loose sand deposits with main focus on liquefaction under saturated condition followed by the review of the recent developments on the application of granular inclusions in the form of stone columns/granular piles as general ground improvement method as well as seismic hazard mitigation measure are presented. This paper combines the soil fabric evolution effect in term of changes in the soil parameters and the densification effect in analyzing the pore pressures for the granular pile reinforced ground.

## Seismic Hazards Associated with Loose Sand Deposits

Loose sand deposits are susceptible to several disturbances under seismic loading due to less strength and stiffness properties. Typical seismic hazards like ground shaking, structural hazards, lateral spreading, liquefaction, etc., are pronounced in loose sand deposits. The other seismic hazards are mainly influenced by the ground shaking at the surface level. As the strong ground motions propagate towards the ground surface, changes in the strength and stiffness of soil deposits (in comparison to bedrock or bottom stiff soil) tend to amplify ground motions. In general, soft soil layers can amplify significantly particular frequencies of motion. In case of very soft soils, the amplitudes may be attenuated but may develop large strains if the imposed stresses approach the strength of the deposits leading other hazards [2]. Further, if the loose sand deposit is under saturated condition, ground shaking induces the increase in the pore water pressure leading to major seismic risk, liquefaction.

### Liquefaction

One of the major consequences of earthquakes is the phenomenon of 'liquefaction'. Significant amount of work has been performed in the last few decades on liquefaction and its evaluation and remediation [3–13]. Liquefaction occurs in saturated loose sandy deposits if subjected to seismic forces. Deposits of loose granular soils get affected by the ground vibrations induced by an earthquake, resulting in large total and differential settlements of the ground surface [3, 6]. In cases where the deposits consist high water table, the tendency to get densified may result in the development of excess hydrostatic pore water pressures of sufficient magnitude to cause liquefaction of the soil, resulting in settlements and tilting of structures [6]. The pore pressure in the soil increases under repeated earthquake forces [7, 8]. Consequently, the effective stress decreases and if its value approaches zero, the deposit loses its strength completely. Even if the effective stresses do not reduce to zero, the ground becomes very soft and large strains, deformations and lateral flows result. Castro [14] distinguishes two different phenomena that were referred to as 'liquefaction' and 'cyclic mobility'. Liquefaction was referred to as complete loss of shear strength and can occur only in loose sands. Cyclic mobility is the gradual increase of cyclic strains without complete loss of shear strength. It could occur in loose to medium dense sands. The different types of ground failures caused by liquefaction may be defined or identified, and vary in intensity, placement in environment, and consequence. They are sand boils, lateral spreads, flow failures, loss of bearing strength and ground oscillations [6].

The liquefaction potential of any given soil deposit is determined by a combination of the properties of soils, environmental factors and characteristics of the earthquake to which they may be subjected to. Simplified techniques based on in situ testing measurements are commonly used to assess seismic liquefaction potential. Liquefaction potential can be evaluated based on various in situ tests like standard penetration tests, cone penetration tests, shear-wave velocity measurements, and Becker penetration test for gravely soils. Most of the simplified charts or equations rely on the analyses of liquefaction case histories. Using empirical, simple regression, or statistical methods, a boundary (liquefaction curve) or classification technique is used to separate the occurrence or non-occurrence of liquefaction. There are different probabilistic and deterministic approaches also in practice for liquefaction hazard assessment. A detailed summary on the different liquefaction evaluation methods and information on magnitude scaling factors, correction factors for overburden pressure, slope of the ground, and input values for earthquake magnitude and peak acceleration, etc., are presented by [7–9].

## Granular Inclusions to Mitigate Seismic Hazards

Soil improvement techniques are employed to mitigate seismic hazards. Most common methods to improve the engineering properties of the soils can be broadly classified as densification, reinforcement, grouting/mixing and drainage. Granular inclusions in the columnar form are of different types viz. sand drains, sand compaction piles; granular piles or stone columns, which are stiffer and stronger that the ambient soil, have been used as a ground improvement technique. This technique aids to increase bearing capacity, reduce settlement, increase the time rate of consolidation, improve stability which mitigate the seismic risks especially enhances the resistance to liquefaction of soft ground. Ground improvement by means of granular piles/stone columns/geopiers, which is associated with partial substitution of the in situ soil, originated in 1960s. Stone columns/granular piles can be adapted to a wide variety of soils as ground improvement method. Loose sandy soils, silty or clayey sands and soils with undrained shear strength within the range 7–50 kPa can use stone columns.

### Materials

Stone columns generally use gravel or crushed stone as backfill. Selection of gravel material for granular pile construction is very important as the performance of the improved system is governed by the granular material. In general, coarse, open-graded stone, of size varying from about 12 to 75 mm, is used [15]. However, the actual size of the granular material depends mainly on the gradation of in situ soil. Saito et al. [16] proposed a formula for selection of the size of the material for stone column in relation to grain size of the surround in situ soil as:

$$20D_{s15} < D_{G15} < 9D_{s85}$$

where $D_{s15}$ and $D_{G15}$ are the sizes/diameters (mm) of soil particles and gravel material, respectively, passing 15 percent and $D_{s85}$ is the diameter of soil passing 85 percent in a grain size analysis test.

### Construction

Theoretical background, analysis, design aspects and installation techniques were being developed since 1970s by various researchers and practicing engineers all over the world [17–20]. Various techniques of installation have been conceived for various types of columnar inclusions in a wide variety of soils such as loose sandy to soft compressible soils depending on technical ability, efficiency and local conditions. Granular piles are installed by vibro-compaction, vibro-replacement, cased bore hole (rammed stone columns/granular piles) or by simple auger boring methods [15, 19, 21, 22].

Vibro-compaction method is applicable for soils with less than 18–20 % fines content. Vibro-compozer method was used in Japan for the installation of granular piles. In India, cased borehole method or ramming stone column method [19] is used for the construction of granular piles. In this method, rammed granular piles are installed into the ground by partial or full displacement methods and by ramming in stages, using a heavy falling weight, within a 'pre-bored casing' or 'driven closed end casing', retracting the casing pipe stepwise. In the latter case, driving of closed end tube itself densifies the surrounding soil. Ramming of granular piles further densifies and reinforces the ground. Granular material is dumped into the hole and rammed by a 15–20 kN rammer in lifts of 1.0–1.5 m keeping the drop height of the rammer is 1.5–2.0 m. After the formation of the full length of the granular pile, it is further rammed with a heavier weight of about 40 kN to recompress the same.

Design

Design of granular piles/stone columns involves the consideration of different mechanisms that are expected to function as per the improvement programme. The primary mechanisms to consider for the design are densification, reinforcement and drainage. The diameter of the granular pile, spacing between the granular piles, pattern of the piles installation, information about the length of the pile (termination depth) and gradation details of the granular material etc. need to be defined in the design process. Barksdale and Bachus [15] presented various design aspects to be considered while designing the stone columns. Priebe and Keller [20] demonstrated the design concepts for vibro replacement. IS 15284 [23] and JGS [22] are the other two good resources to have the concepts for granular piles design. Design curves developed by Seed and Booker [4] are used in general for sizing the granular piles as a liquefaction remediation measure considering the drainage mechanism. To consider the densification effect in connection to liquefaction mitigation, improved SPT N values or cone tip resistance values could be correlated to cyclic resistance ratio and design accordingly [24].

## Recent Research Developments on Granular Piles

Research on granular piles can be broadly classified into for normal ground improvement (non-seismic case) and for liquefaction mitigation (dynamic case). In both the categories studies are being carried through experimental, analytical and numerical works and case studies.

Granular Inclusions Under Non-seismic Case: Developments

Under static case many studies focused on the stone columns/granular piles in soft cohesive soils to observe the failure mechanisms and to understand the group effects. Recent experimental studies in the category are: Black et al. [25] where, it was investigated the use of tubular wire mesh for jacketing the stone columns for improving the peat type of soil. Ambily and Gandhi [26] conducted experimental and FEM based numerical analyses to study the behaviour of stone columns in single and group configuration. Black et al. [27] conducted large triaxial tests to study the settlement performance of the stone column reinforced foundations. As the common mechanism that governs the limiting load is bulging encasement of stone columns is being attempted to enhance the performance of stone columns. In recent years, geosynthetic encased stone columns is the new research area for several researchers [28–34].

The densification effect of granular piles in improving deformation properties of the ambient soil was studied by Murali Krishna and Madhav [35] and Murali Krishna et al. [36]. Murali Krishna and Madhav [35] considered the change of the soil parameters in the zone of influence (unit cell) around the stone columns in terms of linear and exponential variation and evolved simple expressions and charts for finding the equivalent deformation properties of the improved ground. Figure 1 shows the concept of change in deformation properties due to densification effect proposed.

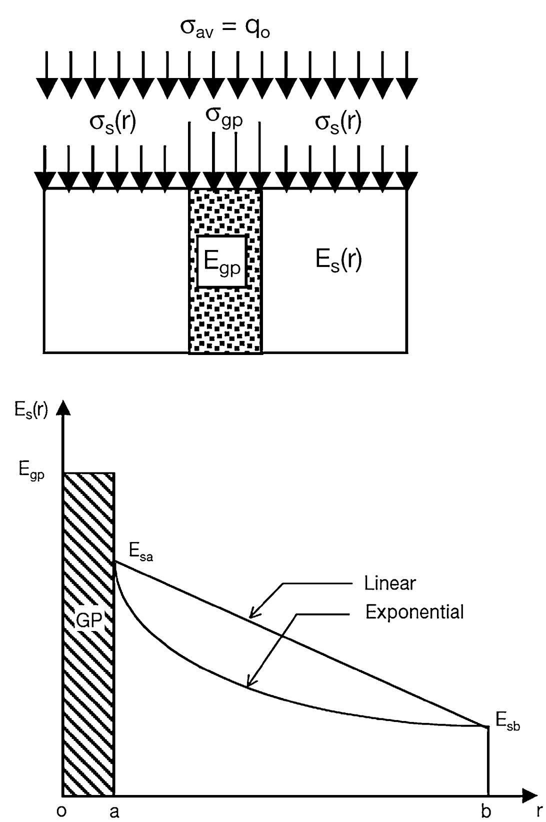


**Fig. 1** Concept of densification effect in changing the deformation properties of granular pile reinforced ground [35]

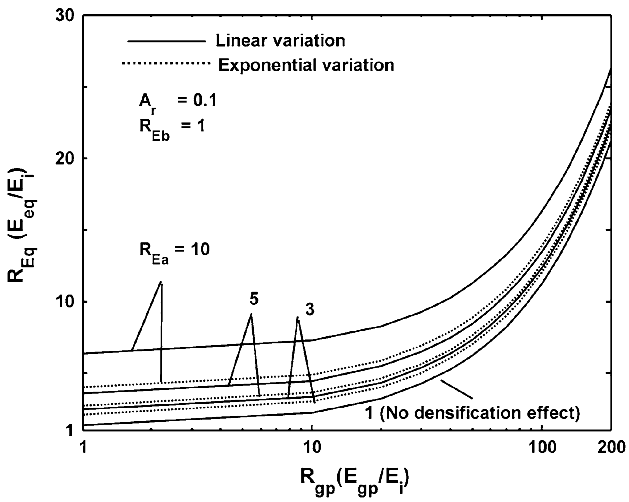


**Fig. 2** Equivalent deformation properties of the improved ground: a typical chart [35]

Typical chart for equivalent deformation properties [35] is presented in Fig. 2. Murali Krishna et al. [36] incorporated similar densification effect in terms of change in deformation moduli in the settlement analysis of the granular pile reinforced ground (Fig. 3). The degree of densification can easily be predicted in terms of improvement in the in situ SPT N values of the treated ground in comparison to the virgin untreated ground. Murali Krishna and Madhav [37] proposed a simple equation, based on the collated field values [38], for predicting the improved SPT N value in terms of the normalised value (SPT $N_1$ value normalised to 100 kPa overburden pressure) as shown in Eq. 1.

$$N_{1\_tr} = N_{1\_untr} + \frac{a_s N_{1\_untr}}{A + B a_s} \tag{1}$$

where $N_{1\_tr}$ is the modified SPT value of the treated soil; $a_s$ is the replacement ratio expressed in percentage; and A and B are the parameters that depend on SPT $N_1$ value of untreated soil ($N_{1\_untr}$) as:

$$A = 1.23\, e^{0.13 N_{1\_untr}} \quad \text{and } B = 0.03\, N_{1\_untr} \tag{2}$$

Equation 1 is applicable for the range of loose to medium sandy soils having $N_{1\_untr}$ values with in the 4–25 as shown in the Fig. 4.

## Granular Inclusions Under Seismic Case: Developments

Granular piles/stone columns function in many ways to enhance the performance and to mitigate the seismic hazard. Though granular piles are efficient in many ways in mitigating the seismic risks, liquefaction mitigation is the main advantage as it is associated with the drainage function which is a very special feature as granular drains. Adalier and Elgamal [39] summarized some of the field case histories on the use of stone columns as liquefaction counter measure in tabular form. An overview of the various mechanisms that function by granular piles in mitigating the liquefaction was presented by Madhav and Murali Krishna [40] and Murali Krishna [13].

Brennen and Madabhushi [41] performed centrifuge tests to verify the effectiveness of the vertical drains in mitigating the liquefaction. Brennen and Madabhushi [42] conducted centrifuge tests to study the liquefaction and drainage in stratified soil with and without vertical drains. Figure 5 shows the typical test configuration considered for centrifuge tests in stratified soil. It was reported that the drains are effectively prevented the sand boiling and the

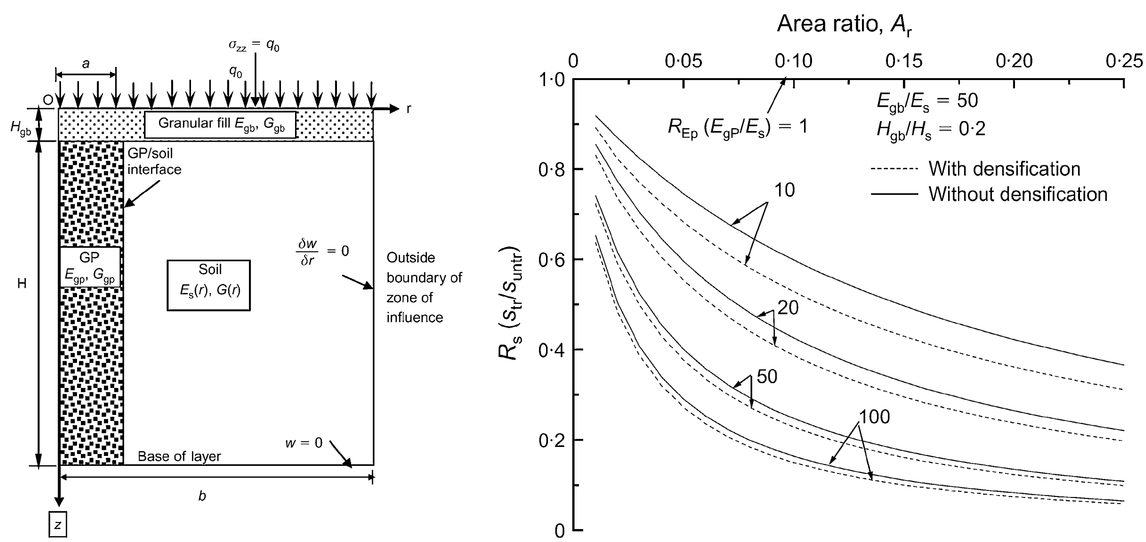


**Fig. 3** Problem considered for the settlement analysis of granular pile reinforced ground and typical result [36]

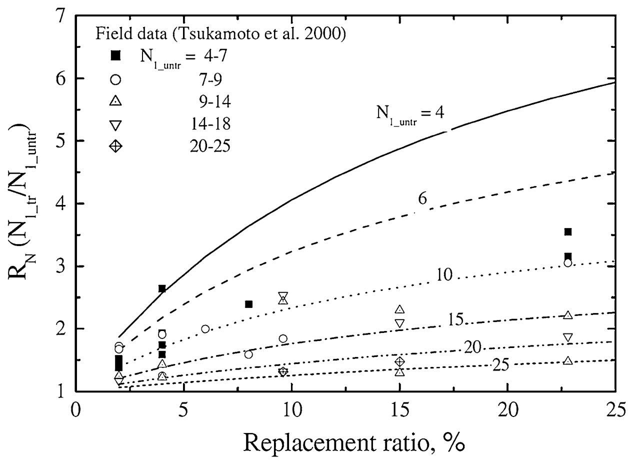


**Fig. 4** Increases in the normalised SPT-$N_1$ values of soil [37]

thin surface fine layers with did not affect the excess pore water pressure response. As drains are employed in groups, Brennen and Madabhushi [43] presented findings from the centrifuge tests exclusively on the group effects considering the drain catchment area at different locations with respect to centre of the group. It was shown from the experimental results that drains with large catchment areas (drains around the edges of groups) perform more poorly than unit cells, and also have a detrimental effect on other drains. Qi-ying et al. [44] carried the shaking table tests to study the liquefaction mitigation of sandy soil using sand pile of different lengths. Figure 6 shows the model configuration considered for the shaking table test and typical pore water pressure recordings during the test at a depth of 300 mm with pile length of 200 mm in the improved case at different pile spacings.

Most of the designs of the granular drains/stone columns for liquefaction mitigation depend on the analytical frame work developed by Seed and Booker [4]. Over the years the original analytical frame work went on various modifications incorporating various other complementary effects of granular inclusions in addition to the drainage effect. Stone columns improve the ground by reinforcement, densification of the surrounding soil apart from providing drainage; they dilate during seismic events generating negative pore water pressure for small instances and provide some storage. Thus the various mechanisms of gravel drains/granular piles in liquefaction mitigation can be listed as drainage, storage, dilation, densification and reinforcement.

Design diagrams by Iai and Koizumi [45] and Onoue [46] incorporated the effects of drain resistance in the analyses of Seed and Booker [4]. Baez [24] presented an evaluation of the relative effectiveness of stone columns for the mitigation of liquefaction of soil. Pestana et al. [47] analysed the development of excess pore pressure in a layered soil profile, accounting for vertical and horizontal drainage with a non-constant ‘equivalent hydraulic conductivity’, and head losses due to horizontal flow into the drain and the presence of a reservoir directly connected to the drain were considered. Boulanger et al. [48] evaluated the drainage capacity of stone columns or gravel drains for

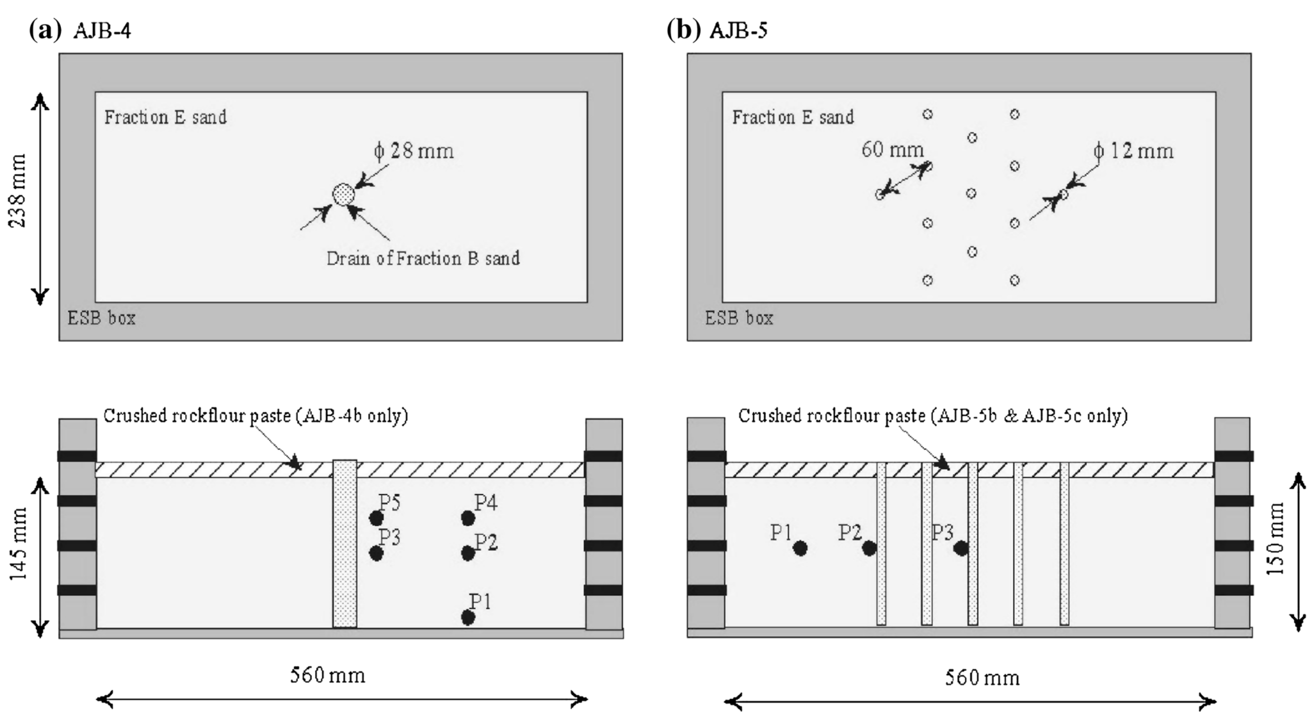


**Fig. 5** Test configurations considered for stratified soil with single and group drains [42]

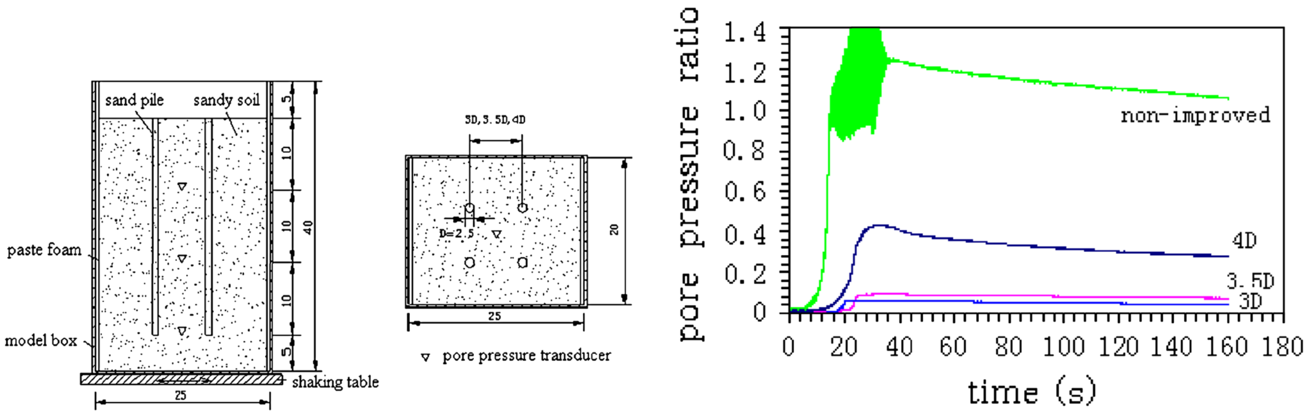


**Fig. 6** Model configuration considered by Qi-ying et al. [44] and typical pore pressure response obtained [44]

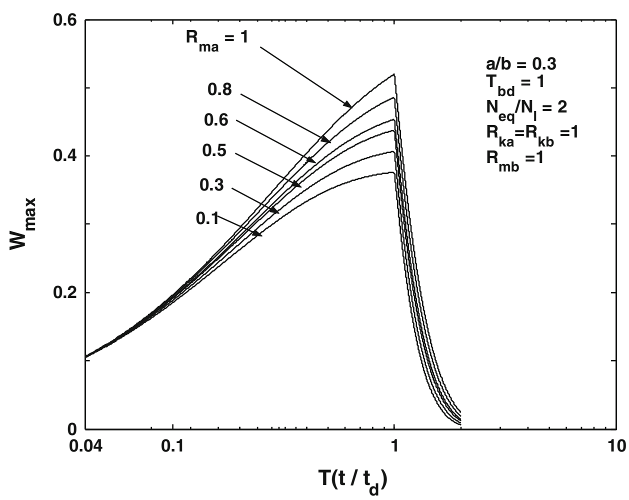


**Fig. 7** Effect of densification at near end with respect to coefficient of volume compressibility ($R_{ma}$) on maximum pore pressure ratio ($W_{max}$) [53]

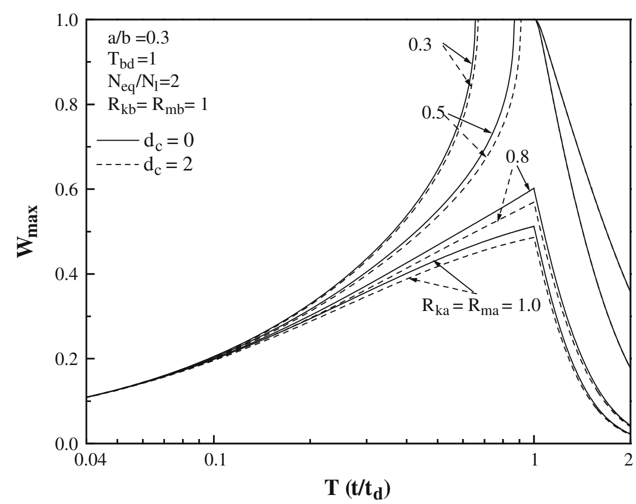


**Fig. 8** Effect of densification with respect to coefficients of permeability and volume compressibility at near end ($R_{ka}$ and $R_{ma}$) and dilation on $W_{max}$ [12]

mitigating liquefaction hazards. Dilation effect of the stone columns, due to densification around and within the stone columns, on the drainage function of granular piles was studied by Madhav and Arlekar [49] by extending the Seed and Booker model [4]. It was shown that the dilation effect on pore pressure dissipation by granular piles for the range of parameters considered is marginal. Poorooshasb et al. [50] demonstrated the effectiveness of inclusion of stone columns in reducing the risk of liquefaction of very loose to loose sandy and silty sand layers using the concept of equivalent permeability. Poorooshasb et al. [51] and Noorzad et al. [52] demonstrated the reinforcement effect of stone columns while analysing their performance during an earthquake. They proposed that the seismic load imposed on the soil is shared between the stone column and the surrounding ground and stone column carries the major load. Murali Krishna et al. [53] studied the densification effect with respect to the coefficients of permeability and volume change at the near and at the farthest ends of the granular pile, individually and together, on maximum pore pressure variations during an earthquake event (Fig. 7). Murali Krishna and Madhav [12] combined both the densification and dilation effects and incorporated them in the analysis of pore pressure generation and dissipation (Fig. 8). They also quantified the effect of type of variation (linear or exponential) of the parameters with distance on maximum pore pressure ratios and concluded that the pore pressures ratios are not sensitive to the type of variation of permeability with distance (Fig. 9). Recently Bouckovalas et al. [54, 55] considered sand fabric evolution effects on drain design for liquefaction mitigation. They proposed that overlooking the shake-down effects of fabric evolution during cyclic loading underestimates the effectiveness of gravel drains.

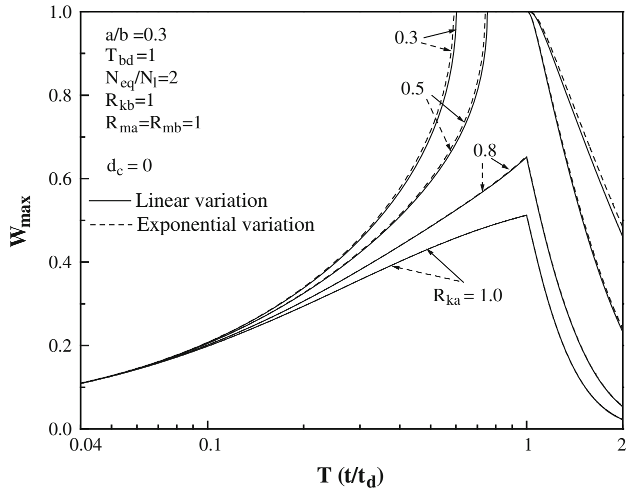


**Fig. 9** Effect of densification with respect to coefficient of permeability near end ($R_{ka}$) on $W_{max}$ for linear and exponential variations

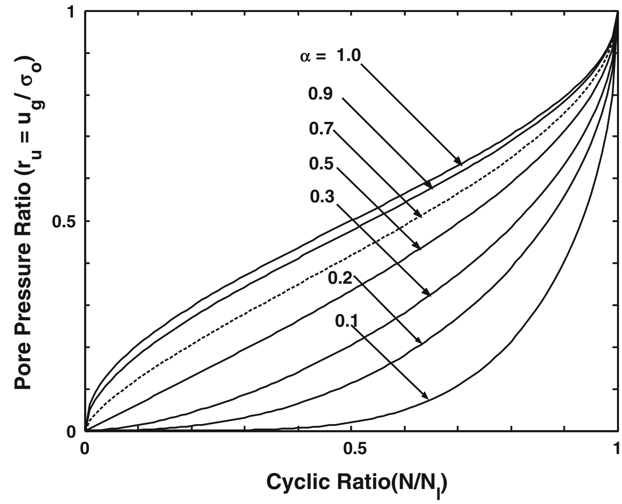


**Fig. 10** Effect of 'α' on pore pressure ratio generation [56]

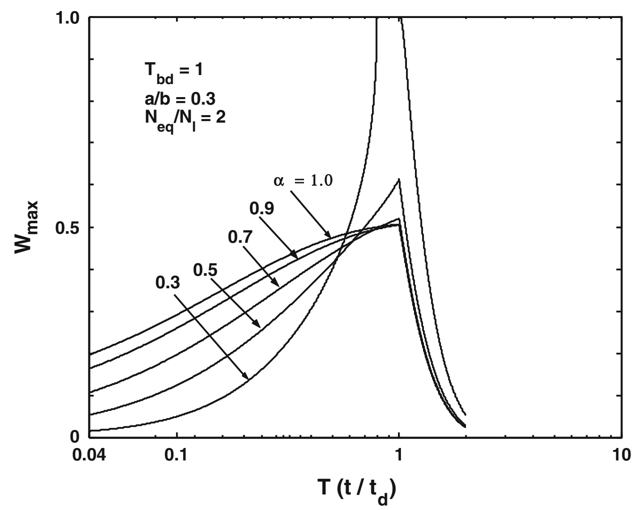


**Fig. 11** Effect of 'α' on maximum pore pressure ratio with no densification and dilation case

## Effect of Rate of Pore Pressure Generation on Maximum Pore Pressure Ratio

Pore pressure generation (Eq. 3) mainly depends on two parameters 'α', an empirical constant which is a function of the soil properties, and $N_l$, number of cycles required to cause liquefaction. In the determination of pore pressure ratio, 'α' value of 0.7 is considered as a typical average value [4].

$$\frac{u_g}{\sigma'_o} = \frac{2}{\pi} \text{arc sin} \left(\frac{N}{N_l}\right)^{1/2\alpha} \tag{3}$$

where $u_g$ is the peak excess hydrostatic pore-water pressure generated by the earthquake; $\sigma'_o$ the initial mean bulk effective stress for triaxial test conditions or the initial vertical effective stress for simple shear conditions; $N$ the number of equivalent cycles induced by the earthquake; $N_l$ the number of such cycles required to cause liquefaction; and α the an empirical constant which is a function of the soil properties. Soil properties change due to improvement of the ground with granular inclusions. It may be necessary to find a new 'α' value for the improved ground. Further, the pore pressure generated by seismic loading is sensitive to relative density of the soil. In this respect number of cycles required to cause liquefaction also depend on relative density [56].

Figure 10 shows the effect of 'α' value on pore pressure generation, in the form of plot between generated pore pressure ratio ($u_g/\sigma'_o$) versus cyclic ratio ($N/N_l$). The rate of pore pressure generation with $N/N_l$ is initially small and the rate becomes very high as $N/N_l$ reaches 1.0 for smaller values of α (α < 0.7). The opposite is true for α > 0.7. The pore pressure increases much faster initially for α values of 0.9 and 1.0. This may be interpreted as the parameter α representing the soil property play major role in generation of pore pressures. It would be interesting to examine if a relation exists between α and $D_r$. Figure 11 shows the effect of 'α' value on variation of maximum pore pressure ratio, $W_{max}$, with '$T$', a non-dimensional time indicating the duration of earthquake. The rate of increase of $W_{max}$ with T is initially small and the rate becomes very high as $T$ reaches 1.0 for smaller values of α (α < 0.7) as observed in Fig. 11 for pore pressure generation. For α values greater than 0.7, $W_{max}$ increases much faster initially but the increase becomes gradual as T reaches 0.1. The peak value of $W_{max}$ increases from about 0.52–0.62 for a decrease in α value of 0.7–0.5. For α value of 0.3, $W_{max}$ increases very sharply, as T reaches 1, and the ground attains liquefaction state ($W_{max} = 1$) at T = 0.8. Peak values of $W_{max}$ are almost the same for α values of 0.9 and 1.0, and are very close (slightly lesser) for α value of 0.7.

## New Model Considering the Soil Fabric Evolution Effect Over Densification Effect

The governing equation for pore pressure generation and dissipation in the ground treated with granular columns following the Seed and Booker [4] formulation but considering densification effect is shown in Eq. 4 [53].

$$\frac{k_h(r)}{\gamma_w \cdot m_v(r)}\left(\frac{1}{r}\frac{\partial u}{\partial r}+\frac{\partial^2 u}{\partial r^2}\right)+\frac{1}{\gamma_w \cdot m_v(r)}\cdot\frac{\partial(k_h(r))}{\partial r}\cdot\frac{\partial u}{\partial r} = \frac{\partial u}{\partial t}-\frac{\partial u_g}{\partial t} \tag{4}$$

$$\frac{\partial u_g}{\partial t}=\frac{\partial u_g}{\partial N}\cdot\frac{\partial N}{\partial t} \tag{5}$$

In Eq. 4 coefficients of permeability and volume change, $k_h(r)$ and $m_v(r)$, are functions of radial distance $r$ from the point of densification (centre of the granular column) and degree of densification. The term $\partial u_g/\partial N$ in Eq. 5 represents the rate of generation of pore pressure during an earthquake event is defined by Eq. 6 according to Seed and Booker [4].

$$\frac{\partial u_g}{\partial N}=\frac{\sigma'_o}{\alpha\pi N_l}\cdot\frac{1}{\sin^{2\alpha-1}\left(\frac{\pi}{2}r_u\right)\cos\left(\frac{\pi}{2}r_u\right)} \tag{6}$$

where $r_u = u/\sigma'_o$ is the pore pressure ratio, $\sigma'_o$ the initial mean bulk effective stress for axi-symmetric conditions or the initial vertical effective stress for simple shear conditions; $N_l$ the number of cycles required to cause liquefaction and α an empirical constant which is a function of the soil properties with typical average value of 0.7. Bouckovalas et al. [54, 55] revised this rate of excess pore pressure generation function (Eq. 6) as

$$\frac{\partial u_g}{\partial N}=\frac{\sigma'_o}{\alpha\pi N_l}\cdot F_1 F_2 \tag{7}$$

where

$$F_1=\frac{1}{(N/N_l)^{1-1/2\alpha}} \quad \text{and } F_2=\frac{1}{\sqrt{1-(N/N_l)^{1/\alpha}}} \tag{8}$$

This revised rate of pore pressure generation function is not a monotonic function of $N/N_l$ but it decreases rapidly in the initial stages of cyclic loading (exclusively controlled by $F_1$); remains constant in the intermediate stage (e.g., $N/N_l = 0.3–0.6$); and at the final stage increases rapidly (exclusively controlled by $F_2$) as shown in the Fig. 12 [55].

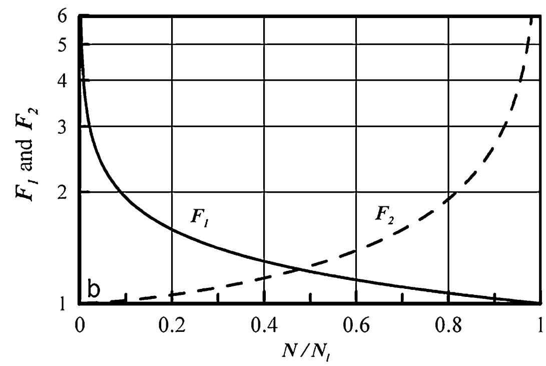


**Fig. 12** Effects of sand fabric evolution ($F_1$) and cyclic shear strain ($F_2$) evolution on the rate of excess pore pressure generation [55]

Further, Bouckovalas et al. [55] considered $F_2$ to be function of current value of excess pore pressure ratio $r_u$. With, $N = t/T_s$ (where $T_s$ is the predominant period of shaking), the final form of Eq. 6 became:

$$\frac{\partial u_g}{\partial N}=\frac{\sigma'_o}{\alpha\pi N_l}\cdot\frac{1}{\left(\frac{t}{T_s N_l}\right)^{1-1/2\alpha}\cos\left(\frac{\pi}{2}r_u\right)} \tag{9}$$

Thus, considering the soil fabric evolution effect [55] for excess pore water pressure generation, the term $\partial u_g/\partial N$ becomes as a function of two terms $F_1$ and as $F_2$ shown in Eqs. 7 and 8 and follows Eq. 9 instead of Eq. 6. With $\partial N/\partial t = N_{eq}/t_d$; and $T_s = t_d/N_{eq}$ Eq. 5 becomes

$$\frac{\partial u_g}{\partial t}=\frac{\sigma'_o}{\alpha\pi\, t_d}\left(\frac{N_{eq}}{N_l}\right)^{1/2\alpha}\cdot\frac{1}{\left(\frac{t}{t_d}\right)^{1-1/2\alpha}\cos\left(\frac{\pi}{2}r_u\right)} \tag{10}$$

with normalized pore pressure $W = u/\sigma'_o$, which is the same as the pore pressure ratio $r_u$ [4], and with $W_g = u_g/\sigma'_o$, Non-dimensionalising the terms $r$ with $R$ (= $r/b$) and $t$ with $T$ (= $t/t_d$), Eq. (4) becomes [57]

$$T_{bd}\cdot\frac{R_k(R)}{R_{mv}(R)}\left(\frac{\partial^2 W}{\partial R^2}+\frac{1}{R}\frac{\partial W}{\partial R}\right)+\frac{T_{bd}\cdot}{R_{mv}(R)}\frac{\partial(R_k(R))}{\partial R}\cdot\frac{\partial W}{\partial R} = \frac{\partial W}{\partial T}-\frac{\partial W_g}{\partial T} \tag{11}$$

where

$$\frac{\partial W_g}{\partial T}=\frac{1}{\alpha\pi}\left(\frac{N_{eq}}{N_l}\right)^{1/2\alpha}\cdot\frac{1}{(T)^{1-1/2\alpha}\cos\left(\frac{\pi}{2}W\right)}$$

$$T_{bd}=\left(\frac{k_{hi}}{\gamma_w}\frac{t_d}{m_{vi}}\right)\cdot\frac{1}{b^2}$$

The non-linear Eq. (11) is solved numerically using a finite difference approach, discretizing the unit cell radially into a number of elements, for the appropriate boundary and initial conditions [57]. It is considered that the material in the drain is far more permeable than the surrounding sand layer (gravel drain is infinitely permeable). So the excess pore-water pressure in the drain is effectively zero i.e., at $r = a$ or $R = a/b$, $u = 0$ or $W = 0$. At the outer boundary of the unit cell, due to symmetry, the pore-water pressure variation in the radial direction is zero, i.e. at $r = \mathrm{b}$ or $R = 1$,

$$\frac{\partial u}{\partial r} = 0 \quad \text{or} \quad \frac{\partial W}{\partial R} = 0 \tag{12}$$

At $t = 0$ or $T = 0$, pore pressures at all the nodes in the soil are equal to the average of pore water pressure generated over the initial time period of $dt$ (or $dT$), i.e., average of pore-water pressure generated over the initial cycle, $dN$, is

$$W_{g\ at\ T=0} = \left(\frac{u_g}{\sigma'_o}\right)_{at\ t=0} = \frac{1}{2}\left(\frac{2}{\pi}\text{arc sin}\left(\frac{dN}{N_l}\right)^{1/2\alpha}\right) \tag{13}$$

The assumptions and limitations associated with the original Seed and Booker [4] model are carried over to the new model also. The smear effect is commonly included through a reduction in the permeability. However, the limitations due to the assumption of infinite permeability for the drain and neglect of the possible clogging of the drain with sediment still remain. Further, assuming the random seismic loading as uniform harmonic loading is another limitation of the method.

Figure 13 shows the comparison of the maximum pore water pressure ratios generated with soil fabric effect [55] and without the soil fabric effect [4]. The figure clearly depicts the effect of soil fabric in reducing the excess pore water pressures very effectively. Figure 14 presents the maximum pore pressure ratio variation with the time for different effects namely: (1) no densification effect and no soil fabric effect, similar to the original Seed and Booker [4] model; (2) densification effect only (considering the change in flow parameters at the near only with $R_{ka} = R_{ma} = 0.8$); (3) soil fabric evolution effect only; and (4) densification effect and soil fabric effects together. $T_{bd} = 1$, $a/b = 0.5$ and $N_{eq}/N_l = 2$ are considered for the purpose. It is seen from the figure that the maximum pore ratios are about 0.64, 0.85, 0.43 and 0.53 for the above effects considered in order, respectively. This implied that the densification effect (considering the change in soil properties) alone raised the maximum pore water pressure ($W_{max}$) by about 30 % and soil fabric effect (consideration of soil state in the form change in pore water pressure generation) reduced the maximum pore water pressure by about 32 % where as the combined effects effectively reduced the $W_{max}$ by about 17 %.

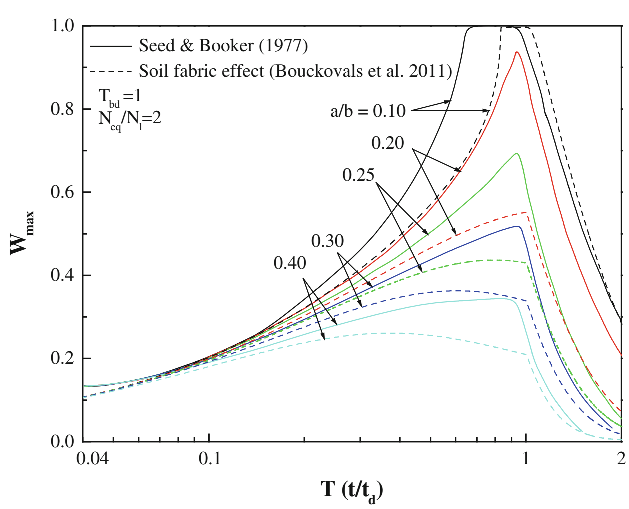


**Fig. 13** Comparison of the maximum excess pore water pressure ratios with and without soil fabric effect

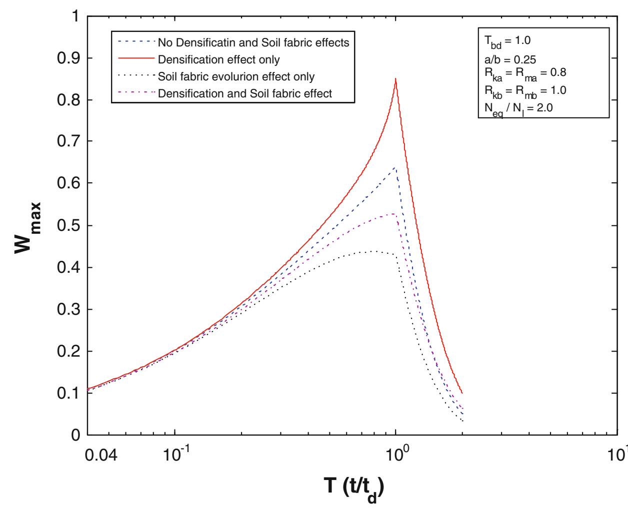


**Fig. 14** Comparison of the maximum excess pore water pressure ratios for different effects

## New Design Curves for Liquefaction Mitigation Using Granular Piles

In many instances, it is required to design the stone columns to prevent liquefaction. Design charts developed by [4] are being extensively used for the purpose. Figure 15 show the variation of the greatest pore pressure ratio $W_{max}$ (peak values of $W_{max}$ observed during the entire period of seismic loading, $T_d$), developed as a function of the spacing ratio, a/b, for values of $N_{eq}/N_l$ equal to 2, and dimensionless time factor $T_{ad} = 10$ and 100 for different cases. For any particular soil and a selected diameter of stone column, $N_{eq}/N_l$ and $T_{ad}$ will be known, and thus, the value of $a/b$ corresponding to allowable value of $W_{max}$ can be read directly from the curves. Figure 15 presents the design curves for different cases for comparison. 'No densification and soil fabric effect' indicates the original Seed and Booker [4] curves while the others with additional effects.

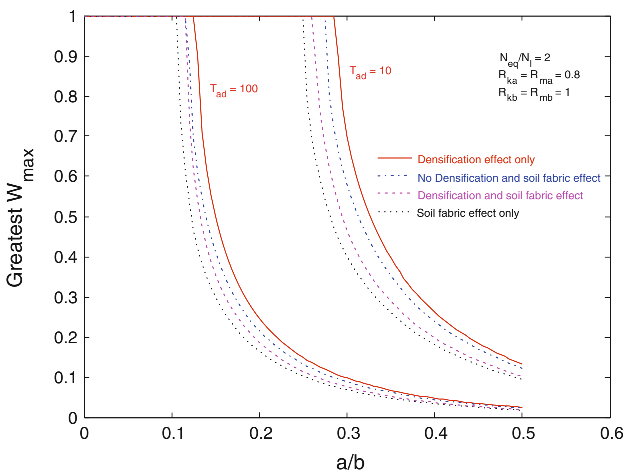


**Fig. 15** Design curves for different cases

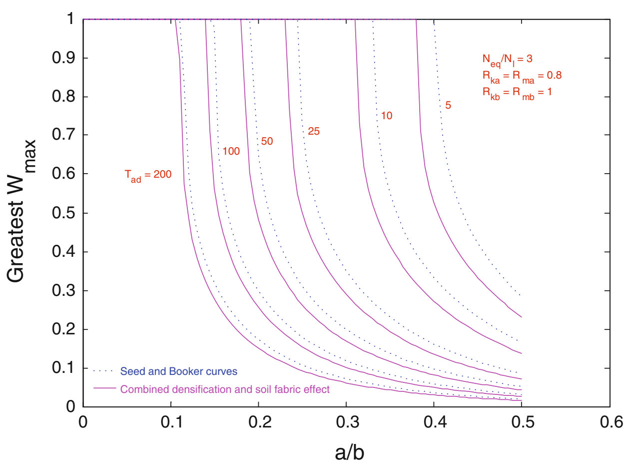


**Fig. 16** Final design curves with combined effect for cyclic ratio ($N_{eq}/N_l$) of 3

It can be observed from the figure that densification effect gives higher *a/b* values which indirectly considers the smear effect while the soil fabric effect alone suggests for lower *a/b* values. The combined effect 'Densification and soil fabric effect', which is more general and realistic in terms of considering most possible effects, gives slightly lower values than that of the Seed and Booker [4] curves. Figures 16 and 17 present the design curves for different cyclic ratio values, $N_{eq}/N_l$ of 3 and 4 respectively. The figures also show the original Seed and Booker [4] curves for comparison. It should be noted that at lower $T_{ad}$ values the difference is very significant.

## Design Example

To demonstrate the procedure of seismic design, consider a soil layer having the properties $k = 10^{-5}$ m/s and

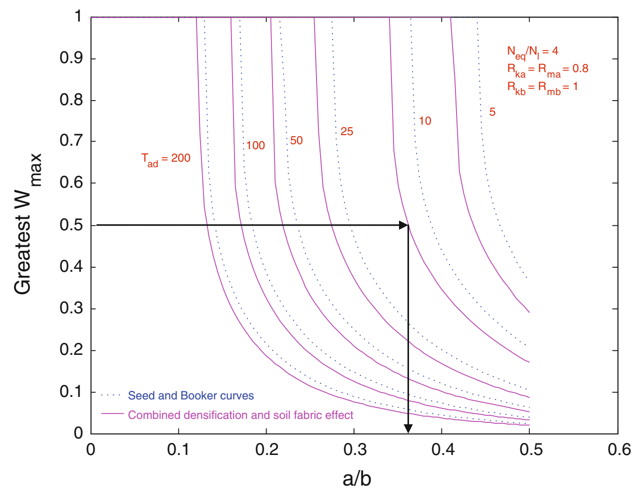


**Fig. 17** Final design curves with combined effect for cyclic ratio ($N_{eq}/N_l$) of 4

$m_v = 6.2 \times 10^{-5}$ kN/m$^2$ is subjected to an earthquake that can be considered as equivalent to 24 uniform stress cycles in a period of 35 s (approximately equivalent to 8.0 magnitude on Richter scale and 0.36 g peak ground acceleration). Under the undrained conditions, say, the soil would liquefy at this sequence of stress application after 6 cycles.

Considering $k = 10^{-5}$ m/s, $m_v = 6.0 \times 10^{-5}$ kN/m$^2$, $N_{eq} = 24$ cycles, $N_l = 6$ cycles, $N_{eq}/N_l = 24/6 = 4$. Assuming diameter of stone column = 0.5 m, radius of stone column, $a = 0.25$ m, $\gamma_w = 9.81$ kN/m$^2$ Dimensionless time factor $T_{ad} = (k/\gamma_w)[t_d/(m_v a^2)] = \left(10^{-5}/9.81\right)\left[35/\left(6.0 \times 10^{-5} \times 0.25^2\right)\right] = 9.5$. If allowable $W_{max} =$ 0.5 (as a design requirement) then, from Fig. 17 (using the curve for combined effect), for $T_{ad} \approx 10$ and $N_{eq}/N_l = 4$, it is obtained that a/b $\geq$ 0.36. For $a/b = 0.36$, $b =$ 0.695 m, diameter of unit cell $D_e = 2 \times b = 1.39$ m and hence spacing of stone columns $= (D_e/1.05) = (1.39/1.05) = 1.32$ m.

The design example presented here illustrates the use of design charts presented to designing the granular pile configuration for the assumed soil and seismic loading conditions. The main limitation of this method is representation of typical random earthquake loading conditions to equivalent uniform harmonic loading conditions. Design earthquake magnitude and the corresponding peak ground acceleration are used for selecting the suitable number of cycles (both total no. of cycles and no. of cycles required for liquefaction) and duration of seismic loading as seismic loading parameters in the design. For the combined densification and soil fabric effect of granular piles, the configuration obtained is 0.5 m dia, at 1.32 m (about 2.6 times dia.) spacing. If the design curve presented for original Seed and Booker case (Fig. 17) is used the required *a/b* value would be around 0.39 and the corresponding diameter and spacing of the granular inclusions are 0.25 and 1.2 m respectively. As, in reality, various mechanisms work together during seismic loading in the ground, improved with installation of granular inclusions, it is recommended to use the combined effect in the analysis and design of granular inclusions as seismic risk mitigation elements.

## Conclusions

Various aspects of ground engineering with granular piles/stone columns for loose saturated sands subjected to seismic loading were discussed in this paper. Discussion on the liquefaction associated with loose sand deposits under saturated conditions along with the outlines of the recent developments on the application of granular inclusions in the form of stone columns/granular piles as general ground improvement method as well as seismic hazard mitigation measure were presented. In general, the design of granular piles for liquefaction mitigation is commonly done using the design charts developed based on analytical model representing pore pressure generation and dissipation considering various effects. Hence various developments in the concepts of the analytical model are briefly discussed. Densification, dilation and soil fabric evolution effects are the recent new considerations in the analysis of pore water pressure generation and dissipation. This paper combined the soil fabric evolution effect and the densification effect in analyzing the pore pressures for the granular pile reinforced ground. The results indicated that densification effect alone raised the maximum pore water pressure by about 30 % and soil fabric effect alone reduced the maximum pore water pressure by about 32 %; whereas the combined effects effectively reduced the same by about 17 %. New design curves were presented considering the soil fabric effect and densification effect and compared with the original Seed and Booker design curves. In reality various mechanisms work together during the seismic loading in ground, improved with installation of granular inclusions. It is recommended to use the combined effect in the analysis and design of granular inclusions as seismic risk mitigation elements. The main limitation of this analytical model is the representation of typical random earthquake loading condition to equivalent uniform harmonic loading conditions. Design earthquake magnitude and the corresponding peak ground acceleration are to be used for selecting the suitable number of cycles (both total no. of cycles and no. of cycles required for liquefaction) and duration for the design. The design example presented above illustrates the same.

## References


1. Seed HB, Idriss IM (1982) Ground motions and soil liquefaction during earthquakes. Earthquake Engineering Research Institute, Oakland
2. PIANC (2006): Seismic design guidelines for port structures, Working Group No. 34 of the Maritime Navigation Commission International Navigation Association, Balkema, Tokyo
3. Martin GR, Finn WDL, Seed HB (1975) Fundamentals of liquefaction under cyclic loading. J Geotech Eng Div ASCE 101(GT5):425–438
4. Seed HB, Booker JR (1977) Stabilization of potentially liquefiable sand deposits using gravel drains. J Geotech Eng Div 103(7): 757–768
5. Seed HB (1979) Soil liquefaction and cyclic mobility evaluation for level ground during earthquakes. J Geotech Eng Div ASCE 105(2):201–255
6. Ishihara K (1993) Liquefaction and flow failure during earthquakes. Geotechnique 42(3):351–415
7. Seed RB, Cetin KO, Moss RES, Kammerer AM, Wu J, Pestana JM, Riemer MF, (2001) Recent advances in soil liquefaction engineering and seismic site response evaluation. In: Proceedings of 4th international conference recent advances in geotechnical earthquake engineering and soil dynamics. San Diego, California, pp 1–45
8. Youd TL, Idriss IM, Ronald DA, Arango I, Castro G, Christian JT, Dobry R, Finn WDL, Harder LF Jr, Hynes ME, Ishihara K, Koester JP, Liao SSC, Marcuson WF III, Martin GR, Mitchell JK, Moriwaki Y, Power MS, Robertson PK, Seed RB, Stokoe KH II (2001) Liquefaction resistance of soils: summary report from the 1996 NCEER and 1998 NCEER/NSF workshops on evaluation of liquefaction resistance of soils. J Geotech Geoenviron Eng 124(10):817–833
9. Idriss IM, Boulanger RW (2005) Evaluation of liquefaction potential, consequences and mitigation. In: Proceedings of Indian Geotechnical Conference. Ahmedabad, India, pp 3–25
10. Sawicki A, Mierczynski J (2006) Developments in modeling liquefaction of granular soils, caused by cyclic loads. Appl Mech Rev Trans ASME 59(3):91–106
11. Madabhushi SPG (2007) Ground improvement methods for liquefaction remediation. Ground Improv 11(4):195–206
12. Murali Krishna A, Madhav MR (2008) Densification and dilation effects of granular piles in liquefaction mitigation. Indian Geotech J 38(3):295–316
13. Murali Krishna A (2011) Mitigation of liquefaction hazard using granular piles. Int J Geotech Earthq Eng 2(1):44–66
14. Castro G (1975) Liquefaction and cyclic mobility of saturated sands. J Geotech Eng Div ASCE 101(6):551–569
15. Barksdale RD, Bachus RC (1983) Design and construction of stone columns, report no. FHWA/RD-83/026, U. S. Department of Transportation, Federal Highway Administration, Washington, DC
16. Saito A, Taghawa K, Tamura T, Oishi H, Nagayama H, Shimaoka H (1987) A countermeasure for sand liquefaction: gravel drain method. Nippon Kokan Technical Report, Overseas No. 51, Japan
17. Hughes JMO, Withers NJ (1974) Reinforcing of soft cohesive soils with stone columns. Ground Eng 7(3):42–49
18. Madhav MR, Iyengar NGR, Vitkar RP, Nandia A (1979) Increased bearing capacity and reduced settlements due to inclusions in soil. In: Proceedings of international conference on soil reinforcement: reinforced earth and other techniques. Paris, 2, pp 329–333
19. Datye KR, Nagaraju SS (1981) Design approach and field control for stone columns. In: Proceedings of 10th international

conference on soil mechanics and foundation engineering. Stockholm, Sweden, 3, pp 637–640
20. Priebe HJ, Keller G (1995) Design of vibro replacement. Ground Eng 28(10):31–37
21. Balaam NP, Booker JR (1981) Analysis of rigid raft supported by granular piles. Int J Num Anal Methods Geomech 5(4):379–403
22. The Japanese Geotechnical Society (JGS) (1998) Remedial measures against soil liquefaction. A.A. Balkema, Rotterdam
23. IS 15284 (Part 1) (2003) Design and construction for ground improvement—guidelines, part 1. Stone columns, analysis. Bureau of Indian Standards, New Delhi
24. Baez JI, (1995) A design model for the reduction of soil liquefaction by vibro-stone columns. PhD thesis, University of Southern California, Los Angeles, CA
25. Black J, Sivakumar V, Madhav M, Hamill GA (2007) Reinforced stone columns in weak deposits: laboratory model study. J Geotech Geoenviron Eng 133(9):1154–1161
26. Ambily AP, Gandhi SR (2007) Behavior of stone columns based on experimental and FEM analysis. J Geotech Geoenviron Eng 133(4):405–415
27. Black J, Sivakumar V, Bell A (2011) The settlement performance of stone column foundations. Geotechnique 61(11):909–922
28. Raithel M, Kirchner A, Schade C, Leusink E (2005) Foundation of constructions on very soft soils with geotextile encased columns—state of the art, Geotechnical Special Publication, No. 130–142, Geo-Frontiers 2005, 1867–1877
29. Park SS, Lee DY, Yoo C, Jung ST, Lee BR (2006) Development of geogrid reinforced stone column method, Rep. No. 05-C17, Korea Institute of Construction and Transportation Technology Evaluation and Planning, Seoul, 134
30. Malarvizhi SN, Ilamparuthi K (2006) Behavior of geogrid encased stone column and stone column stabilized soft clay bed. In: Proceedings of 6th international conference on physical modelling in geotechnics. pp 1489–1494
31. Murugesan S, Rajagopal K (2007) Model tests on geosynthetic encased stone columns. Geosynth Int 24:346–354
32. Wu CS, Hong YS (2008) Laboratory tests on geosynthetic-encapsulated sand columns. Geotext Geomembr 27:107–120
33. Gniel J, Bouazza A (2009) Improvement of soft soils using geogrid encased stone columns. Geotext Geomembr 27(3):167–175
34. Yoo C (2010) Performance of geosynthetic-encased stone columns in embankment construction: numerical investigation. J Geotech Geoenviron Eng 136(8):1148–1160
35. Murali Krishna A, Madhav MR (2007) Equivalent deformation properties of ground treated with rammed granular piles. Int J Geotech Eng 1(1):31–38
36. Murali Krishna A, Madhav MR, Madhavi Latha G (2007) Densification effect of granular piles on settlement response of treated ground. Ground Improv 11(3):127–136
37. Murali Krishna A, Madhav MR (2009) Treatment of loose to medium dense sands by granular piles: improved SPT N1 values. Geotech Geol Eng 27:455–459
38. Tsukamoto Y, Ishihara K, Yamamoto M, Harada K, Yabe H (2000) Soil densification due to static sand pile installation for liquefaction remediation. Soils Found 40(2):9–20
39. Adalier K, Elgamal A (2004) Mitigation of liquefaction and associated ground deformations by stone columns. Eng Geol 72(3–4):275–291
40. Madhav MR, Murali Krishna A (2008) Liquefaction mitigation of sand deposits by granular piles—an overview. In: Liu H, Deng A, Chu J (eds) Geotechnical engineering for disaster mitigation and rehabilitation. Proceedings of 2nd international conference for disaster mitigation and rehabilitation, Nanjing, China, pp 66–79
41. Brennan AJ, Madabhushi SPG (2002) Effectiveness of vertical drains in mitigation of liquefaction. Soil Dyn Earthq Eng 22(9):1059–1065
42. Brennan AJ, Madabhushi SPG (2005) Liquefaction and drainage in stratified soil. ASCE J Geotech Geoenviron Eng 131(7):876–885
43. Brennan AJ, Madabhushi SPG (2011) Drain groups in liquefiable soil. Int J Geotech Earthq Eng 2(1):67–82
44. Qi-ying N, Yong-juan W, Wei-ze Y (2008) Shaking table tests on liquefiable sandy soil reinforced by different length pile. In: Proceedings of 14th world conference on earthquake engineering, Beijing, China, Paper No. 04-02-0126
45. Iai S, Koizumi K (1986) Estimation of earthquake induced excess pore water pressure for gravel drains. In: Proceedings of 7th Japan Earthquake Engineering. Symposium, pp 679–684
46. Onoue A (1988) Diagrams considering well resistance for designing spacing ratio of gravel drains. Soils Found 28(3):160–168
47. Pestana JM, Hunt CE, Goughnour RR, Kammerer AM (1998) Effect of storage capacity on vertical drain performance in liquefiable sand deposits. In: Proceedings 2nd international conference on ground improvement techniques, Singapore, pp 373–380
48. Boulanger R, Idriss I, Stewart D, Hashash Y, Schmidt B (1998) Drainage capacity of stone columns or gravel drains for mitigating liquefaction. In: Proceedings, geotechnical earthquake engineering and soil dynamics III, Special Publication No. 75. vol I, pp 678–690
49. Madhav MR, Arlekar JN (2000) Dilation of granular piles in mitigating liquefaction of sand deposits. In: 12th world conference earthquake engineering, Auckland. No: 1035 (CD-ROM)
50. Poorooshasb HB, Noorzad A, Miura N, Madhav MR (2000) Prevention of earthquake induced liquefaction of sandy deposits using stone columns. In: Proceedings of international symposium on Lowland Technology 2000. Saga pp 213–220
51. Poorooshasb HB, Madhav MR, Noorzad A (2006) Performance of stone columns subjected to a seismic base excitation. In: Proceedings of international symposium on Lowland Technology-2006. Saga, pp 1189–1194
52. Noorzad A, Poorooshasb HB, Madhav MR (2007) Performance of partially penetrating stone columns during an earthquake. In: Proceedings of 10th symposium on numerical models in geomechanics (NUMOG X). Rhodes, Greece, pp 503–508
53. Murali Krishna A, Madhav MR, Madhavi Latha G (2006) Liquefaction mitigation of ground treated with granular piles: densification effect. ISET J Earthq Technol 43(4):105–120
54. Bouckovalas GD, Papadimitriou AG, Niarchos D (2009) Gravel drains for the remediation of liquefiable sites: the Seed & Booker (1977) approach revisited. In: Proceedings of the keynote lecture, IS-Tokyo 2009
55. Bouckovalas GD, Papadimitriou AG, Niarchos D, Tsiapas YZ (2011) Sand fabric evolution effects on drain design for liquefaction mitigation. Soil Dyn Earthq Eng 31:1426–1439
56. Murali Krishna A (2003) Liquefaction mitigation of loose sand deposits by rammed granular piles. M. Tech thesis, Indian Institute of Technology, Kanpur, India
57. Kumar K (2012) Study on design aspects of stone columns and liquefaction mitigation. M. Tech thesis, Indian Institute of Technology Guawhati, Guwahati, India